# Immobilized stem–loop structured probes as conformational switches for enzymatic detection of microbial 16S rRNA

**Benjamin Bockisch, Thomas Grunwald[1], Edzard Spillner and Reinhard Bredehorst***

Institut für Biochemie und Lebensmittelchemie, Abteilung für Biochemie und Molekularbiologie, Universität Hamburg, Martin-Luther-King-Platz 6, 20146 Hamburg, Germany and [1]PLS-Design GmbH, Eichenstrasse 42, 20255 Hamburg, Germany

## ABSTRACT

**We have designed and evaluated novel DNA stem–loop structured probes for enzymatic detection of nucleic acid targets. These probes constitute a novel class of conformational switches for enzymatic activity, which in the absence of a target sterically shield an affinity label and upon hybridization of the target to the recognition sequence that forms the loop of the probe restore accessibility of the label for the binding of a reporter enzyme. Analysis of probe characteristics revealed stem stability as the most important parameter governing detection functionality, while other factors such as the length of linker molecules attaching the label to the stem–loop structure and the nature of the solid support proved to be less critical. Apparently, the bulky nature of the reporter enzyme facilitates shielding of the label in the absence of the target, thereby conferring considerable structural tolerance to the conformational switch system. The stem–loop structured probes allow sensitive detection of unlabeled nucleic acid targets. Employing a microtiter assay format, 4 ng of bacterial 16S ribosomal RNA corresponding to 8 fmol could be detected, which can be compared favorably with current immobilized molecular beacon concepts based on fluorescence detection.**

## INTRODUCTION

For the detection of nucleic acid targets, stem–loop structured oligonucleotide probes are superior to linear probes in several aspects. Most important is their ability to detect unlabeled nucleic acid targets and to provide greatly improved mismatch discrimination. For these reasons, stem–loop probes have rapidly been adopted for a variety of solution-based applications such as the real-time detection of PCR amplicons (1), mRNA detection in living cells (2), single nucleotide polymorphism and mutation detection (3,4), identification of pathogens (5) and fluorescence *in situ* hybridization (6). However, there are also several reports on surface-immobilized stem–loop structures for the design of DNA microarrays and biosensors (7–12).

The vast majority of stem–loop structured oligonucleotide probes utilize a novel implementation of fluorescence energy transfer. These structures known as 'molecular beacons' contain a target sequence flanked by short self-complementary segments and are labeled on either ends with a fluorophore and a corresponding quencher (1). In their unbound state they assume a stem–loop conformation, bringing fluorophore and quencher into close proximity and thus extinguishing fluorescence through non-radiative energy transfer. On target binding, the stem–loop structure opens, increasing the distance between the labels and thereby restoring fluorescence. Immobilized beacons, however, show a fluorescence enhancement of only $\sim$2–5 (8,10–13), much less than the enhancement factor of 25–200 observed in solution (1,2,14,15). As a result, immobilized molecular beacons do not provide the sensitivity desirable for DNA microarrays and biosensors.

Recently, an electrochemical DNA sensor that employs immobilized stem–loop structured oligonucleotide probes containing a terminal ferrocene label as the conformational switch has been reported (16). In the absence of a target, the electrochemically active label is close to the electrode surface generating redox current and upon target hybridization the label is separated from the electrode abolishing the exponentially distance-dependent electron transfer process. The sensor allows sensitive detection of oligodeoxynucleotides without the use of exogenous reagents, but represents a 'signal-off' device since hybridization abolishes the redox current. 'Signal-off' sensors, however, pose a major limitation in that they are highly susceptible to false-positive responses

*To whom correspondence should be addressed. Tel: +49 40 42838 2840; Fax: +49 40 42838 7255; Email: bredehorst@chemie.uni-hamburg.de
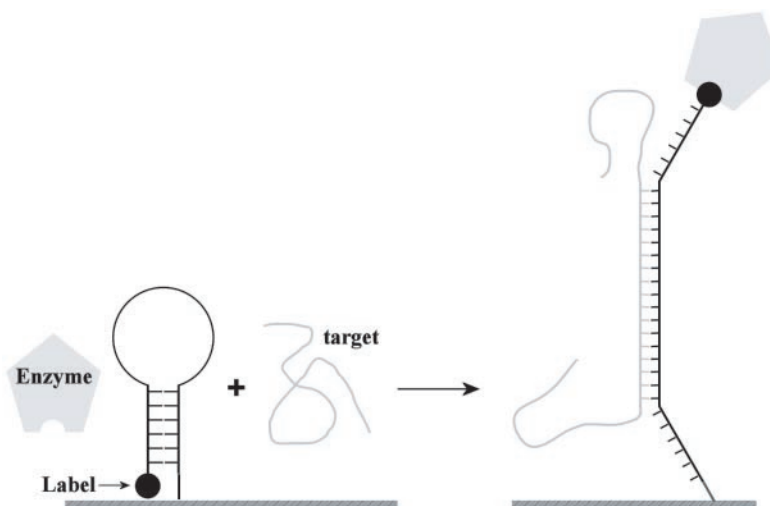
**Figure 1.** Principle of the enzymatic conformational switch system. In the closed conformation the affinity label is sterically shielded, inaccessible to the reporter enzyme. On target binding, the hairpin opens, making the label available for enzyme binding.

(16). In this study, we designed an alternative 'signal-on' sensor for the detection of nucleic acid targets utilizing stem–loop structured oligodeoxynucleotide probes that are immobilized through one terminus and carrying an affinity label at the other. In the absence of a target, the closed conformation of the probe forces the label into close proximity to the surface of the solid support rendering it inaccessible to detector molecules (Figure 1). Upon target hybridization, the probe switches to a linear conformation, thereby restoring accessibility of the label. Employing conjugates with an enzymatic moiety for the detection of exposed label residues, this novel conformational switch system allows detection of unlabeled nucleic acid targets in the low pM range. In addition to sensitive target detection, the system provides a high degree of versatility regarding the applicability of different labels and reporter molecules for optical and electrochemical detection.

## MATERIALS AND METHODS

### Oligonucleotides

Oligodeoxynucleotides employed in this study are listed in Table 1, and were synthesized by Metabion (Martinsried, Germany) and Sigma-ARK (Darmstadt, Germany). A mixed DNA–RNA–oligonucleotide (MB1-6-rC) was synthesized by Thermo (Ulm, Germany).

Oligodeoxynucleotide MB1-B6-ARP was synthesized from MB1-6-rC. MB1-6-rC (1 nmol) was incubated in 20 μl of 10 mM NaIO$_4$ in the dark for 40 min at 4°C, and for a further 30 min at 37°C after the addition of 5 μl of 100 mM Na$_2$S$_2$O$_3$ to remove excess periodate. After the addition of 50 μg ARP [$N$-(aminooxyacetyl)-$N'$-(D-biotinoyl) hydrazine, trifluoro-acetic acid salt; Molecular Probes, Eugene, OR] in 5 μl H$_2$O, incubation was continued for 1 h at 37°C. The product (MB1-B6-ARP) was purified by ethanol precipitation.

### Preparation of bacterial RNA samples

Total RNA was isolated from *Escherichia coli* TG1 using the standard procedures (17). Total RNA samples of other

**Table 1.** Utilized stem–loop structures and target deoxyoligonucleotides

| | |
|---|---|
| MB1-6-rC | NH$_2$-ggccgt TACTCCCTTCCTCCCCGC acggc-rC |
| MB1-B3 | NH$_2$-cgt TACTCCCTTCCTCCCCGC acg-biotin |
| MB1-B4 | NH$_2$-ccgt TACTCCCTTCCTCCCCGC acgg-biotin |
| MB1-B5 | NH$_2$-gccgt TACTCCCTTCCTCCCCGC acggc-biotin |
| MB1-B6 | NH$_2$-ggccgt TACTCCCTTCCTCCCCGC acggcc-biotin |
| MB1-B6-ARP | NH$_2$-ggccgt TACTCCCTTCCTCCCCGC acggcc-ARP-biotin |
| MB1-B6-TEG | NH$_2$-ggccgt TACTCCCTTCCTCCCCGC acggcc-TEG-biotin |
| MB1-B7 | NH$_2$-cggccgt TACTCCCTTCCTCCCCGC acggccg-biotin |
| MB1-B8 | NH$_2$-gcggccgt TACTCCCTTCCTCCCCGC acggccgc-biotin |
| MB1-B9 | NH$_2$-cgcggccgt TACTCCCTTCCTCCCCGC acggccgcg-biotin |
| MB1-D6 | Digoxigenin-ggccgt TACTCCCTTCCTCCCCGC acggcc-biotin |
| MB2 | NH$_2$-ggccgt CCCAACATTTCACAACAC acggcc-biotin |
| MB3 | NH$_2$-ggccgt CCCCTGCTTTGGTCCGTA acggcc-biotin |
| MB4 | NH$_2$-ggccg TACCGTACTCTAGCTCA cggcc-biotin |
| T1 | GCGGGGAGGAAGGGAGTA |
| T-MB1-0 | GTACTTTCAGCGGGGAGGAAGGGAGTAAAGTTAATA |
| T-MB1-1 | GTACTTTCAGCGGGGAGGAAGGGAGTGAGGTTAATA |
| T-MB1-2 | GTACTTTCAGCGGGGAGGAAGGCAGAAGAGTTAATA |

For stem–loop probes MB1-MB4, upper case denotes the recognition sequence and lower case nucleotides form the stem. Oligodeoxynucleotides were derivatized and labeled using standard attachment chemistry. Terminal amino groups were attached via C6-linker molecules, terminal digoxigenin residues via amide linkage to C6-linker molecules and terminal biotin residues via C3-ether-glycerol linker molecules (for ARP-biotin and TEG-biotin, see Figure 4). rC denotes cytidin.

bacterial species were kindly provided by B. Elsholz (Fraunhofer ISIT, Germany). Isolated RNA was fragmented by the addition of 0.25 vol of 200 mM Tris–acetate, pH 8.1, 500 mM KOAc and 150 mM MgOAc per volume of the sample, followed by incubation for 10 min at 95°C (17). Samples were subsequently cooled on ice and diluted to desired assay concentrations in 5× SSC buffer (75 mM sodium citrate, pH 7.0 and 750 mM NaCl).

### Immobilization of amino-modified stem–loop structures

Amino-modified stem–loop structures were immobilized on epoxy-functionalized microtiter plates (DNA-Immobilizer™, Exiqon, Vedbaek, Denmark). To each well

80 μl of a 1 nM (unless otherwise indicated) solution of amino-biotin-labeled oligodeoxynucleotide in carbonate buffer (100 mM, pH 9.6) was added and the plate incubated overnight at 4°C. Wells were washed thrice with 0.5× SSC–Tween buffer [7.5 mM sodium citrate, pH 7.0, 75 mM NaCl and 0.1% (v/v) Tween-20] prior to use.

### Immobilization of biotin-modified stem–loop structures

Biotin-modified stem–loop structures were immobilized on microtiter plates precoated with streptavidin (Streptavidin Immobilizer™, Nunc, Wiesbaden, Germany). To each well, 80 μl of a 1 nM solution of biotin-digoxigenin-labeled oligodeoxynucleotide in PBS buffer (10 mM phosphate, pH 7.4 and 137 mM NaCl) was added and the plate incubated overnight at 4°C. Wells were washed thrice with 0.5× SSC–Tween prior to use.

### Colorimetric assay

Nucleic acid sample in 100 μl 5× SSC buffer was added to each well, coated with amino- or biotin-modified stem–loop structures, and incubated for 90 min at 22°C. After washing thrice with ice-cold 0.5× SSC–Tween buffer, 100 μl of the appropriate AP conjugate (ExtrAvidin–AP or anti-Dig–$F_{ab}$-fragment–AP) diluted 1:1000 in ice-cold 5× SSC buffer was added. Following the incubation for 10 min at 4°C, wells were again washed thrice with 0.5× SSC–Tween buffer and 100 μl of the chromogenic AP-substrate pNPP (5 mg/ml in 10 mM Tris, pH 9.5 and 137 mM NaCl) was added to each well. Absorption of each well at 405 nm was measured at 60 s intervals on a Tecan GENIOS microplate reader and the change of extinction per unit time recorded.

### Chemiluminescent stem–loop probe assays

Chemiluminescent assays were carried out in opaque white microtiter plates precoated with streptavidin (Streptavidin Immobilizer™, Nunc, Wiesbaden, Germany). Biotin-digoxigenin-labeled oligodeoxynucleotide (1 nM, 110 μl) in PBS buffer was added to each well and the plate incubated overnight at 4°C. Wells were washed thrice with 0.5× SSC–Tween buffer prior to use. Nucleic acid sample in 120 μl of 5× SSC buffer was added to each well and incubated for 90 min at 22°C. After washing thrice with ice-cold 0.5× SSC–Tween buffer, 120 μl of anti-Dig–$F_{ab}$–AP conjugate, diluted 1:1000 in ice-cold 5× SSC buffer, was added. Following the incubation for 10 min at 4°C, wells were again washed thrice with 0.5× SSC–Tween buffer. Substrate working solution [120 μl; CSPD, BM Chemiluminescence ELISA Substrate (AP), Roche Diagnostics, Penzberg, Germany] was added to each well, incubated for 10 min at 22°C and the total light emission of each well was measured on a GENIOS microplate reader (Tecan, Crailsheim, Germany) using 'maximum dynamic range' mode.

## RESULTS

For proof-of-principle a DNA stem–loop structure was constructed containing a stem of complementary 6 nt segments (MB1-B6; Table 1), a loop recognition sequence complementary to an 18 nt segment of the 16S rRNA of *E.coli*, a biotin label at the 3′-terminus and a primary amino group at the

5′-terminus for immobilization of the stem–loop structure onto epoxy-functionalized microtiter wells (Figure 1). Utilizing a oligodeoxynucleotide (18 nt) complementary to the loop recognition sequence (oligodeoxynucleotide T1, Table 1) as the target and a conjugate of ExtrAvidin and alkaline phosphatase (AP) for detection of exposed biotin residues, initial experiments showed a signal-to-background ratio of 10 (data not shown). Since these data demonstrated the feasibility of using immobilized stem–loop structures as conformational switches for enzymatic activity, the impact of several parameters including stem length, accessibility of the biotin label for the ExtrAvidin–AP conjugate in the absence of target molecules, use of alternative labels as well as properties of the solid support carrying the immobilized stem–loop structures, was investigated to optimize this novel approach for the sensitive detection of microbial RNA targets.

### Effect of stem length

Seven variants of MB-stem–loop structures varying only in the stem length (B3-B9 variants of MB1, Table 1) were constructed to evaluate the effect of stem stability on background and target detection. As evident from the data in Figure 2, background signals showed a significant increase with decreasing stem length and increasing incubation periods in the presence of ExtrAvidin–AP conjugate. These data suggest that open stem–loop structures that bind the ExtrAvidin–AP conjugate are removed from the equilibrium between the open and closed
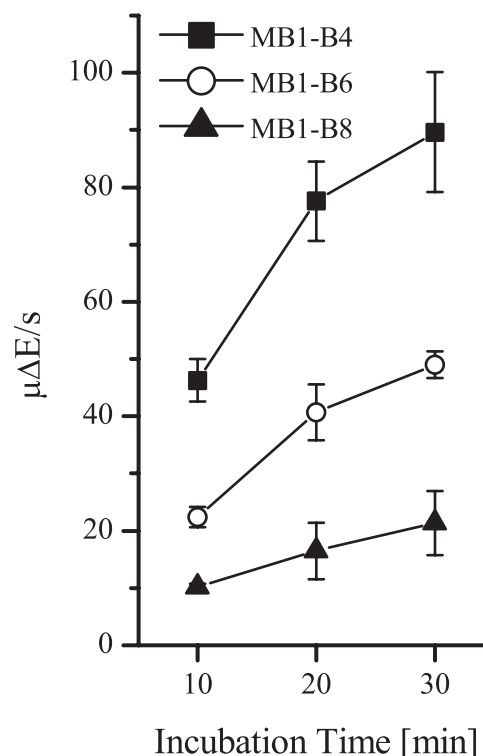


**Figure 2.** Effect of stem length and incubation time on background level. Employing a colorimetric assay with ExtrAvidin–AP as reporter conjugate, signal levels obtained with stem–loop structures MB1-B4 (closed squares), MB1-B6 (open circles) and MB1-B8 (closed triangles) in the absence of the target were determined. Shown are mean values ± SD obtained from four experiments.
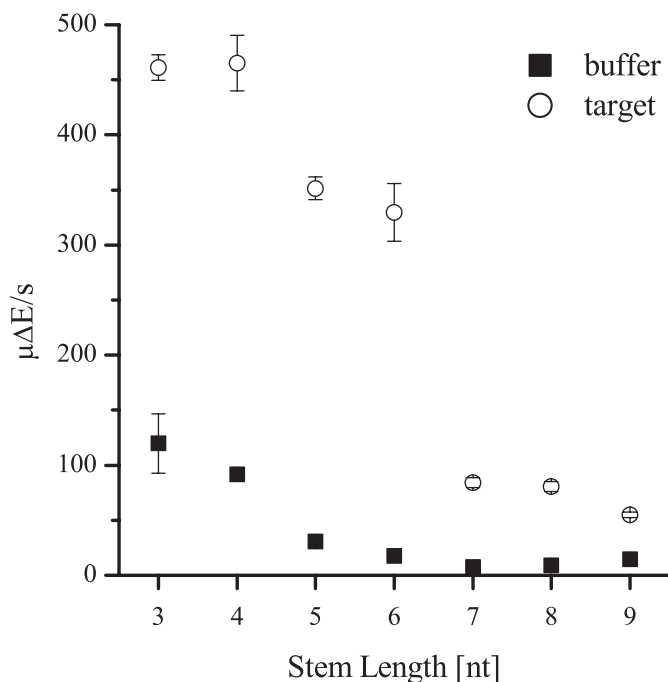
**Figure 3.** Effect of stem length on signal and background values. Employing a colorimetric assay with ExtrAvidin–AP as the reporter conjugate, signal levels in the absence (closed squares) and presence (open circles) of target T1 (1 nM) were determined for stem–loop structures with a stem length varying from 3 to 9 (MB1-B3 to MB1-B9). Shown are mean values ± SD obtained from four experiments.

forms as the bulky conjugate sterically hinders reformation of the closed stem–loop conformations. As a result, open stem–loop structures carrying the conjugate accumulate slowly, causing the background signal to increase proportional to incubation time. In the presence of the target, (oligodeoxynucleotide T1, Table 1) corresponding results were obtained. As shown in Figure 3, stem lengths ≤6 nt generated a strong signal, while longer stems were too stable to allow efficient opening of the stem–loop structure in the presence of the target. Since stems of 5 nt and shorter also exhibited a marked increase in background signal, a stem length of 6 nt provides the optimal background-to-signal ratio. Thermal treatment (50, 70 and 95°C) of the various immobilized stem–loop structures prior to hybridization did not lead to any significant enhancement of the signal even when the target was present at a concentration of 10 nM (data not shown). Apparently, loop closure reactions are too highly favored over target-loop hybridization reactions.

### Effect of label attachment

Since efficient steric shielding of the biotin residues in closed loop structures is essential for low background values, the optimal length of the chemical linker attaching biotin to the 3′-terminus of stem–loop structures was evaluated. The routinely applied C3-linker was compared with a shorter (ARP-linker) and a longer (TEG-linker) version (Figure 4). As shown in Figure 5, the most extended TEG-linker generated the highest background signal, but absolute differences in background signals were minor. However, in the presence of
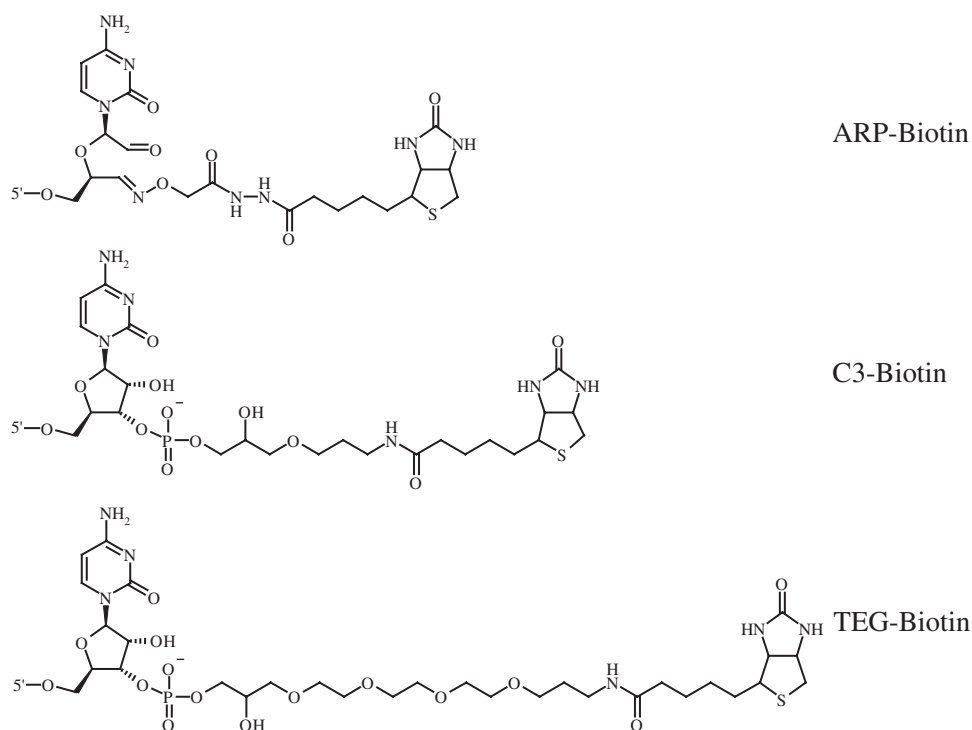


**Figure 4.** Structure of linker molecules employed for biotin attachment to the stem–loop structures. ARP-biotin [*N*-(aminooxyacetyl)-*N'*-(D-biotinoyl)hydrazine] is attached via Schiff base chemistry to an aldehyde group generated by oxidative cleavage of the terminal ribose moiety of cytidin (rC). C3-Biotin contains a C3-ether-glycerol linker attached to the biotin residue via an amide bond. In TEG-biotin, the C3-ether-glycerol linker is extended by a triethyleneglycol (TEG) moiety.
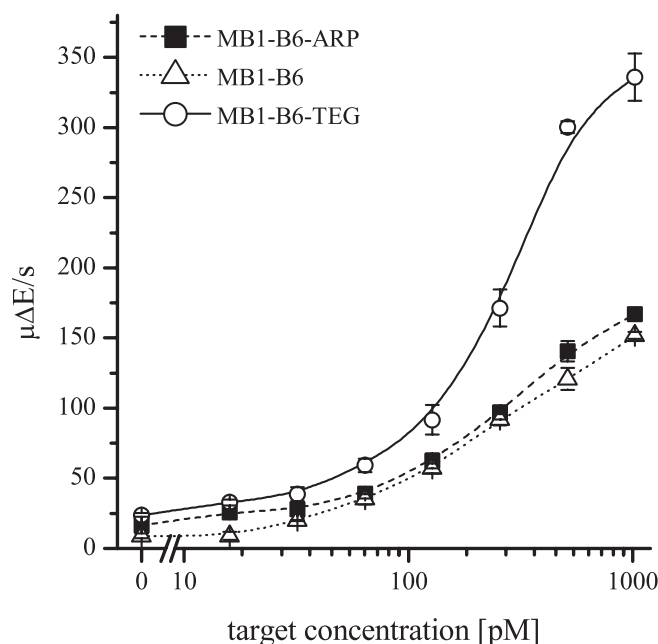
**Figure 5.** Effect of biotin attachment on detection sensitivity. Employing a colorimetric assay with ExtrAvidin–AP as the reporter conjugate, the detection sensitivity of target T1 with stem–loop structures MB1-B6-ARP (closed squares), MB1-B6 (open triangles) and MB1-B6-TEG (open circles) was compared. Shown are mean values ± SD obtained from four experiments.



**Figure 6.** Effect of probe density on the signal-to-background ratio. (A) Microtiter wells coated with varying concentrations of stem–loop structure MB1-B6 were used to determine signal levels in the absence (closed circles) and presence (open triangles) of target T1 (1 mM) employing a colorimetric assay with ExtrAvidin–AP as the reporter conjugate. Shown are mean values ± SD obtained from four experiments. (B) The signal-to-background ratios calculated from these data.

high target concentrations, the TEG-linker provided markedly higher signal levels than the other two linker molecules. These data demonstrate that accessibility of the label for reporter enzyme conjugates in the open conformation is as important as efficient steric shielding of the label in closed loop structures.

### Application of different labels

To evaluate the suitability of other labels, affinity systems and different solid supports for the conformational switch principle, a stem–loop structure corresponding to MB1-B6 in sequence but labeled at the 3′-terminus with biotin and at the 5′-terminus with digoxigenin (MB1-D6, Table 1) was immobilized onto a streptavidin-coated surface via the biotin label. Digoxigenin served as the sterically quenchable label and enzymatic detection was performed with an anti-digoxigenin–$F_{ab}$–AP conjugate. Signal enhancement factors determined with this hapten/antibody affinity pair were comparable to those obtained with the biotin/ExtrAvidin–AP conjugate system. For example, comparative detection of the target oligodeoxynucleotide T1 (10 nM) by stem–loop structures MB1-B6 and MB1-D6 generated signal enhancement factors of 17.6 ± 1.7 for the biotin/ExtrAvidin system and 18.5 ± 1.4 for the digoxigenin/anti-digoxigenin–$F_{ab}$ system. These data indicate that other labels as well as protein-coated surfaces are also suitable to establish efficient conformational switch assay systems.

### Density of stem–loop structures

Since the level of both background and signal depends on the number of immobilized stem–loop structures, the effect of
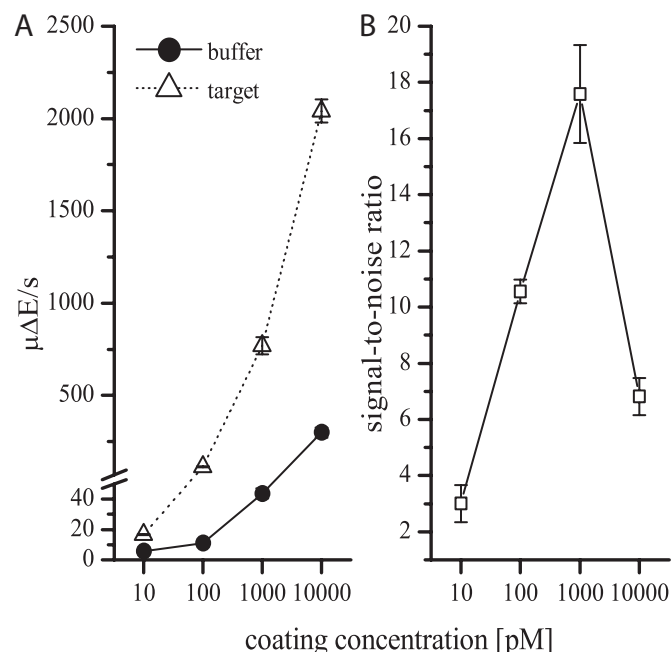
different densities of stem–loop structures on the detection sensitivity was analyzed utilizing stem–loop structure MB1-B6 and target oligodeoxynucleotide T1. Figure 6A shows both the signal and background rising considerably as the density of stem–loop structures increases. The signal-to-noise ratio, however, reaches a maximum at a coating concentration of 1 nM, followed by a steep decrease at a coating concentration of 10 nM (Figure 6B).

### Detection of bacterial ribosomal 16S RNA

16S ribosomal RNA is a fairly bulky molecule (1541 bp in *E.coli*) with a complex secondary structure. We employed three methods to reduce the potentially inhibitory effects of the secondary structure on the detection sensitivity: the use of chaperone probes designed to disrupt local secondary structure by binding to intramolecular hybridization sites (18), thermal denaturation and catalytic fragmentation. Of these, only fragmentation of the target allowed detection of ribosomal RNA.

Employing digoxigenin as a label and a chemiluminescent substrate for the detection of bound anti-digoxigenin–$F_{ab}$–AP conjugates, <10 ng total fragmented *E.coli* RNA generated a detectable signal (Figure 7). Since 10 ng of total *E.coli* RNA contain ~4 ng 16S ribosomal RNA, the detection level of 16S ribosomal RNA is in the range of 60–70 pM. Utilizing oligodeoxynucleotide T1 (Table 1) as the target, the detection level is, under otherwise identical conditions, 6- to 7-fold lower (10 pM, data not shown). These data suggest that even fragmented 16S ribosomal RNA poses some sterical constraints for efficient hybridization to immobilized hairpin structures resulting in a reduced detection sensitivity of 16S RNA.
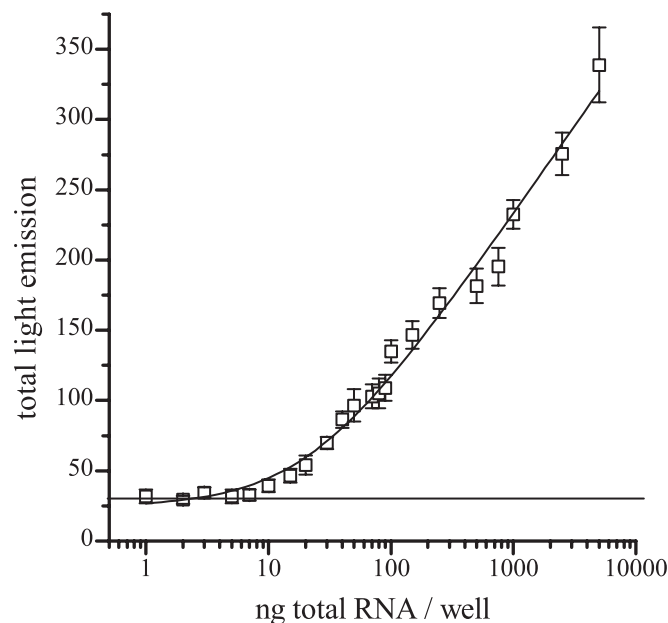
**Figure 7.** Detection of fragmented *E.coli* 16S ribosomal RNA. Employing stem–loop structure MB1-D6 and anti-digoxigenin–$F_{ab}$–AP as the reporter conjugate in a chemiluminescent assay, the detection sensitivity of fragmented *E.coli* 16S ribosomal RNA was determined. Shown are mean values ± SD of replicates from five independent experiments. The horizontal bar marks the background signal (buffer control).
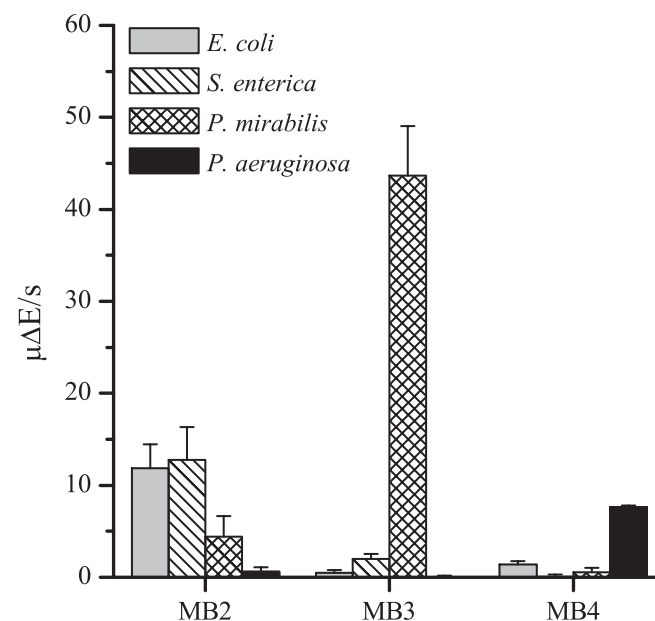


**Figure 8.** Detection of pathogen-specific 16S ribosomal RNA. A colorimetric assay with ExtrAvidin–AP as the reporter conjugate was employed to detect fragmented 16S ribosomal RNA from *E.coli* (gray bars), *Salmonella enterica* (striped bars), *Proteus mirabilis* (chequered bars) and *Pseudomonas aeruginosa* (closed bars) with stem–loop structures MB2, MB3 and MB4. Hybridization was carried out in 5× SSC/50% formamide. Specificities: MB2, *Enterobacteriaceae* (*E.coli*, *S.enterica*); MB3, *Proteus* spp.; MB4, *P.aeruginosa*. Shown are mean values ± SD obtained from four experiments.

To confirm the viability of the conformational switch concept as a bioanalytical tool, the newly developed technology was applied toward the detection of different bacterial strains. Three stem–loop structures of different specificity were employed in a colorimetric assay to detect and identify fragmented 16S ribosomal RNA from four bacterial species. As shown in Figure 8, each of the employed stem–loop structure is capable of specifically detecting the corresponding target sample. Results obtained for MB2 show that a partial signal (∼40% of the signal for perfectly matched RNA from *E.coli* and *Salmonella enterica*) is obtained for *Proteus mirabilis* RNA, which differs from the target sequence in a single position, while the doubly mismatched *Pseudomonas aeruginosa* RNA is not detected. These findings suggest that the conformational switch system is able to discriminate analytes mismatched in more than one position. This is supported by experiments with mismatched oligonucleotide targets, which also show that doubly mismatched targets do not generate significant signals (Figure 9).

The assay's capability to detect minute amounts of target in a mixture is demonstrated by the specific detection of fragmented RNA from either *P.mirabilis* or *P.aeruginosa* in samples containing large excess amounts of fragmented *E.coli* RNA in addition to the target RNAs (Table 2). The constant signal levels indicate that the stem–loop structures are not influenced by a high background of non-target nucleic acid, allowing specific detection in mixtures containing as little as 0.1% of target.

## DISCUSSION

In this study, we have designed novel DNA stem–loop structured probes for enzymatic detection of nucleic acid targets.
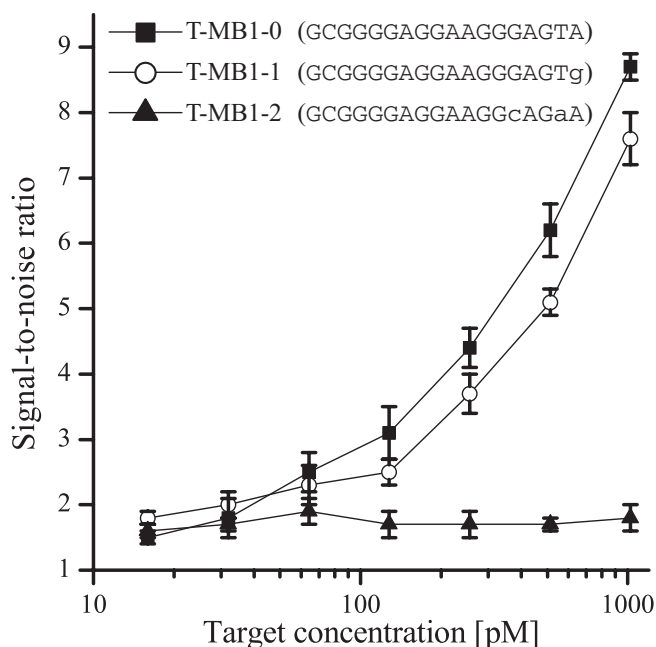


**Figure 9.** Discrimination of mismatches. Employing a colorimetric assay with ExtrAvidin–AP as the reporter conjugate, signal levels obtained with stem–loop structure MB1-B6 in the presence of varying amounts of partially mismatched target were determined. Targets: T-MB1-0 (perfect match), T-MB1-1 (single mismatch) and T-MB1-2 (double mismatch); recognition sequences are shown in the figure (mismatched bases in lower case); for full sequence of target oligonucleotides see Table 1. Hybridization was carried out in 5× SSC/50% formamide. Shown are mean values ± SD obtained from four experiments.

**Table 2.** A colorimetric assay with ExtrAvidin–AP as reporter conjugate was employed to detect fragmented 16S ribosomal RNA from *P.mirabilis* (*P.m.*) or *P.aeruginosa* (*P.a.*) in a mixture containing fragmented total RNA from both *P.mirabilis* and *P.aeruginosa* (0.2 μg each) and excess amounts of fragmented *E.coli* (*E.c.*) total RNA (1–200 μg)

| Detection of *P.mirabilis* in the presence of *E.coli* | | Detection of *P.aeruginosa* in the presence of *E.coli* | |
|---|---|---|---|
| Ratio *P.m./E.c.* | μΔ*E*/s ± SD | Ratio *P.a./E.c.* | μΔ*E*/s ± SD |
| 1:5 | 35 ± 1 | 1:5 | 13 ± 1 |
| 1:25 | 36 ± 2 | 1:25 | 12 ± 1 |
| 1:100 | 33 ± 2 | 1:100 | 12 ± 2 |
| 1:1000 | 39 ± 8 | 1:1000 | 13 ± 1 |

Hybridization was carried out in 5× SSC/50% formamide. Shown are mean values ± SD obtained from four experiments.

These probes constitute a novel class of conformational switches relying on steric shielding of an affinity label in the absence of a target and exposure of the affinity label upon hybridization of target to a recognition sequence in the loop of the probe. Recently, a conformational switch system based on ferrocene has been reported, which offers significant advantages over optically detected molecular beacons owing to low cost/mass/power requirements of electrochemical detection (19), and the relatively high stability and environmental insensitivity of electroactive labels (16). However, this system is inherently limited by its 'signal off' nature and the intrinsic susceptibility to false-positive response. In contrast, the system described in this study includes an enzymatic 'signal on' detection step that is capable of amplifying the signal-on target binding. Employing microtiter plates, ~1 fmol (10 pM) of oligodeoxynucleotides and ~8 fmol (66 pM) of fragmented 16S ribosomal RNA could be detected. This sensitivity matches that of the electrochemical DNA sensor (16) and exceeds that of fluorescence-based immobilized molecular beacons by at least one order of magnitude (20). Considering the relatively large assay volume of microtiter plates, miniaturization of the sensor platform is likely to improve the sensitivity significantly. Coupled with more specialized sensor systems, detection of 16S ribosomal RNA samples in the sub-picomolar range should be feasible.

Basic structural considerations governing molecular beacon design also apply to the newly designed probes. Stem length has a major influence on the performance of the probe. As with molecular beacons (21), short stems (<5 nt) easily hybridize with the target. The efficiency of shielding of the affinity label, however, is reduced considerably due to low thermodynamic stability of the stem–loop structure even in absence of the target, leading to increased background values. Longer stems (>6 nt), while generating low background on account of high stability, show only weak signals in the presence of the target, most probably due to inefficient disruption of the secondary structure by target molecules. Thermal opening of longer stems prior to hybridization showed no effect, presumably due to fast reforming of the stem–loop structure. Stems of 5–6 nt seem to offer the best balance between high signal level and low background values.

As demonstrated in this study, the novel conformational switch concept is suitable for different affinity systems and solid support characteristics. Preliminary results obtained with mercapto-modified stem–loop structures immobilized on glass

or gold suggest that these materials commonly used in biochip and microarray applications are also suitable for this detection system. Apparently, utilization of reporter enzymes for detection of exposed label residues confers considerable tolerance to sterical requirements for efficient shielding of the affinity label in the absence of the target. Binding of a large detection complex to an affinity label can be more easily prevented than the fluorescence of molecular beacons. This also explains the relatively moderate impact of the length of linker molecules attaching the affinity label to the stem–loop probe on background binding of reporter enzyme conjugates in the absence of the target.

In summary, the new probe technology allows sensitive detection of nucleic acid targets. Owing to the use of reporter enzymes, the technology is suitable for various combinations of different affinity systems, detection methods and solid support materials, and is equally applicable for optical and electrochemical detection. Furthermore, based on preliminary experiments with stem–loop probes on electrochemical microdevices (22), our novel conformational switch system can be easily adapted to microarray systems.

## REFERENCES

1. Tyagi,S. and Kramer,F.R. (1996) Molecular beacons: probes that fluoresce upon hybridization. *Nat. Biotechnol.*, **14**, 303–308.
2. Sokol,D.L., Zhang,X., Lu,P. and Gewirtz,A.M. (1998) Real time detection of DNA.RNA hybridization in living cells. *Proc. Natl Acad. Sci. USA*, **95**, 11538–11543.
3. Kostrikis,L.G., Tyagi,S., Mhlanga,M.M., Ho,D.D. and Kramer,F.R. (1998) Spectral genotyping of human alleles. *Science*, **279**, 1228–1229.
4. Piatek,A.S., Tyagi,S., Pol,A.C., Telenti,A., Miller,L.P., Kramer,F.R. and Alland,D. (1998) Molecular beacon sequence analysis for detecting drug resistance in *Mycobacterium tuberculosis*. *Nat. Biotechnol.*, **16**, 359–363.
5. Vet,J.A., Majithia,A.R., Marras,S.A., Tyagi,S., Dube,S., Poiesz,B.J. and Kramer,F.R. (1999) Multiplex detection of four pathogenic retroviruses using molecular beacons. *Proc. Natl Acad. Sci. USA*, **96**, 6394–6399.
6. Xi,C., Balberg,M., Boppart,S.A. and Raskin,L. (2003) Use of DNA and peptide nucleic acid molecular beacons for detection and quantification of rRNA in solution and in whole cells. *Appl. Environ. Microbiol.*, **69**, 5673–5678.
7. Brown,L.J., Brown,T., Cummins,J. and Hamilton,A. (2000) Molecular beacons attached to glass beads fluoresce upon hybridization to target DNA. *Chem. Commun. (Camb.)*, **7**, 621–622.
8. Fang,X., Liu,X., Schuster,S. and Tan,W. (1999) Designing a novel molecular beacon for surface-immobilized DNA hybridization studies. *J. Am. Chem. Soc.*, **121**, 2921–2922.
9. Du,H., Disney,M.D., Miller,B.L. and Krauss,T.D. (2003) Hybridization-based unquenching of DNA hairpins on au surfaces: prototypical 'molecular beacon' biosensors. *J. Am. Chem. Soc.*, **125**, 4012–4013.
10. Liu,X., Farmerie,W., Schuster,S. and Tan,W. (2000) Molecular beacons for DNA biosensors with micrometer to submicrometer dimensions. *Anal. Biochem.*, **283**, 56–63.
11. Wang,H., Li,J., Liu,H., Liu,Q., Mei,Q., Wang,Y., Zhu,J., He,N. and Lu,Z. (2002) Label-free hybridization detection of a single nucleotide mismatch by immobilization of molecular beacons on an agarose film. *Nucleic Acids Res.*, **30**, e61.

12. Yao,G. and Tan,W. (2004) Molecular-beacon-based array for sensitive DNA analysis. *Anal. Biochem.*, **331**, 216–223.

13. Liu,X. and Tan,W. (1999) A fiber-optic evanescent wave DNA biosensor based on novel molecular beacons. *Anal. Chem.*, **71**, 5054–5059.

14. Tan,W., Fang,X., Li,J. and Liu,X. (2000) Molecular beacons: a novel DNA probe for nucleic acid and protein studies. *Chemistry*, **6**, 1107–1111.

15. Bonnet,G., Tyagi,S., Libchaber,A. and Kramer,F.R. (1999) Thermodynamic basis of the enhanced specificity of structured DNA probes. *Proc. Natl Acad. Sci. USA*, **96**, 6171–6176.

16. Fan,C., Plaxco,K.W. and Heeger,A.J. (2003) Electrochemical interrogation of conformational changes as a reagentless method for the sequence-specific detection of DNA. *Proc. Natl Acad. Sci. USA*, **100**, 9134–9137.

17. Ausubel,F.M. (1987) *Current Protocols in Molecular Biology*. Greene Pub. Associates and Wiley-Interscience J. Wiley, NY.

18. Small,J., Call,D.R., Brockman,F.J., Straub,T.M. and Chandler,D.P. (2001) Direct detection of 16S rRNA in soil extracts by using oligonucleotide microarrays. *Appl. Environ. Microbiol.*, **67**, 4708–4716.

19. Bard,A.J. and Faulkner,L.R. (2001) *Electrochemical Methods: Fundamentals and Applications, 2nd edn*. Wiley, NY.

20. Gaylord,B.S., Heeger,A.J. and Bazan,G.C. (2002) DNA detection using water-soluble conjugated polymers and peptide nucleic acid probes. *Proc. Natl Acad. Sci. USA*, **99**, 10954–10957.

21. Tsourkas,A., Behlke,M.A., Rose,S.D. and Bao,G. (2003) Hybridization kinetics and thermodynamics of molecular beacons. *Nucleic Acids Res.*, **31**, 1319–1330.

22. Nebling,E., Grunwald,T., Albers,J., Schafer,P. and Hintsche,R. (2004) Electrical detection of viral DNA using ultramicroelectrode arrays. *Anal. Chem.*, **76**, 689–696.